Dispersed multiphase flows: From Stokes suspensions to turbulence

Kyongmin Yeo

Lawrence Berkeley National Laboratory

EARTH SCIENCES DIVISION

August 14, 2012

Thanks to: Martin R. Maxey (Brown University)

Dispersed multiphase flows

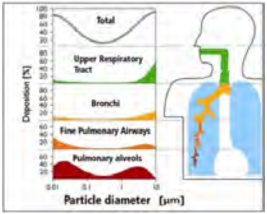

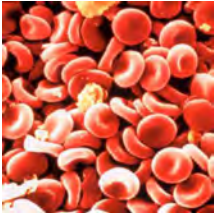

Range of scales

- Reynolds number: ratio of viscous timescale to inertial timescale

$$Re_b = \frac{\rho \mathcal{U} \mathcal{L}}{\mu}$$

- Cloud: $Re_b \sim O(10^5) - O(10^6)$
- Human respiratory system: $Re_b \sim O(10^{-1}) - O(10^3)$
- Blood flow: $Re_b \sim O(10^{-3}) - O(10^2)$
- Microfluidic devices: $Re_b \sim O(10^{-3}) - O(1)$

Range of scales

- Reynolds number: ratio of viscous timescale to inertial timescale

$$Re_b = \frac{\rho \mathcal{U} \mathcal{L}}{\mu} \qquad Re_p = \frac{\rho a^2 \dot{\gamma}}{\mu}$$

- Cloud: $Re_b \sim O(10^5) - O(10^6)$
  $a \sim O(1) - O(10^2)\mu m$, $Re_p \sim O(10^{-1}) - O(10)$.
- Human respiratory system: $Re_b \sim O(10^{-1}) - O(10^3)$
  $a \leq O(10)\mu m$, $Re_p \sim O(10^{-2}) - O(1)$.
- Blood flow: $Re_b \sim O(10^{-3}) - O(10^2)$
  $a \sim O(1)\mu m$, $Re_p \sim O(10^{-4}) - O(1)$.
- Microfluidic devices: $Re_b \sim O(10^{-3}) - O(1)$
  $a \sim O(1)\mu m$, $Re_p \sim O(10^{-4}) - O(10^{-1})$.

- Stokes layer thickness: $l_{St} \sim 1/Re_p$
  $\Rightarrow$ Particle-scale dynamics in Stokes regime,
  while bulk flow can be Stokes to Turbulent flow.

Examples of phase changes in dispersed flows

- Sea-atmosphere interaction

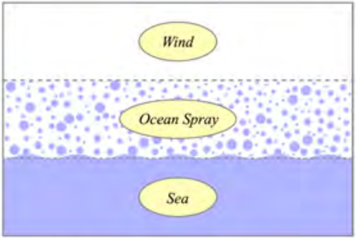

Figure 4. The Lighthill "sandwich model" of a tropical hurricane

Barenblatt (2009)

- Sediment transport

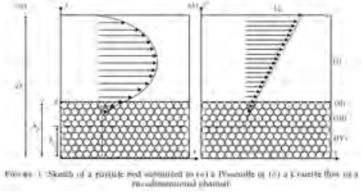

Ouriemi *et al.* (2009)

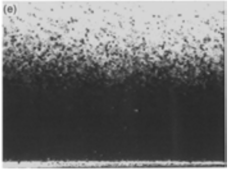

Tripathi & Acrivos (1999)

- Solid boundary
- Boundary layer of concentrated suspensions
- Dilute turbulent dispersed flows

Outline

Review of Lagrangian point-particle model[1]

- Equation of motion for a spherical particle in unsteady flow (Maxey & Riley 1983):

$$
\begin{aligned}
m_p \frac{d\boldsymbol{V}}{dt} =& (m_p - m_f)\boldsymbol{g} + m_f \frac{D\boldsymbol{u}}{Dt} - \frac{m_f}{2}\frac{d}{dt}\left\{\boldsymbol{V} - \boldsymbol{u} - \frac{1}{10}a^2\nabla^2\boldsymbol{u}\right\} \\
& - 6\pi a\mu\left\{\boldsymbol{Q} + a\int_0^t \frac{d\boldsymbol{Q}}{d\tau}\left[\pi\nu(t-\tau)\right]^{-1/2} d\tau\right\} \\
\boldsymbol{Q} =& \boldsymbol{V} - \left(1 + \frac{1}{6}a^2\nabla^2\right)\boldsymbol{u}
\end{aligned}
$$

[1] Balachandar & Eaton *ARFM* (2010)

Review of Lagrangian point-particle model[1]

- Equation of motion for a spherical particle in unsteady flow (Maxey & Riley 1983):

$$m_p \frac{d\boldsymbol{V}}{dt} = (m_p - m_f)\boldsymbol{g} - 6\pi a\mu(\boldsymbol{V} - \boldsymbol{u}) = \boldsymbol{F}$$

- Phase-coupling through drag force $\boldsymbol{F}$;

$$\rho_f \left\{ \frac{\partial \boldsymbol{u}}{\partial t} + (\boldsymbol{u} \cdot \boldsymbol{\nabla})\boldsymbol{u} \right\} = \boldsymbol{\nabla} \cdot \boldsymbol{\sigma} - \boldsymbol{F}, \quad \sigma_{ij} = -p\delta_{ij} + 2\mu_f e_{ij}$$

$\Rightarrow$ Underestimates turbulent attenuation, particularly for $a \geq \eta$.
$\Rightarrow$ Unresolved local distortion of flow field around the particles.

[1] Balachandar & Eaton *ARFM* (2010)

Review of Lagrangian point-particle model[1]

- Equation of motion for a spherical particle in unsteady flow (Maxey & Riley 1983):

$$m_p \frac{d\boldsymbol{V}}{dt} = (m_p - m_f)\boldsymbol{g} - 6\pi a \mu(\boldsymbol{V} - \boldsymbol{u}) = \boldsymbol{F}$$

- Phase-coupling through drag force $\boldsymbol{F}$;

$$\rho_f \left\{ \frac{\partial \boldsymbol{u}}{\partial t} + (\boldsymbol{u} \cdot \boldsymbol{\nabla})\boldsymbol{u} \right\} = \boldsymbol{\nabla} \cdot \boldsymbol{\sigma} - \boldsymbol{F}, \quad \sigma_{ij} = -p\delta_{ij} + 2\mu_f e_{ij}$$

$\Rightarrow$ Underestimates turbulent attenuation, particularly for $a \geq \eta$.
$\Rightarrow$ Unresolved local distortion of flow field around the particles.

- Bulk deviatoric stress in a suspension of force-free particles (Batchelor 1970)

$$\Sigma_{ij} = 2\mu \langle E_{ij} \rangle - \frac{1}{V}\rho_f \int u_i' u_j' dV + \frac{1}{V}\sum_i \int_{\partial\Omega_i} -\mu(u_i n_j + u_j n_i) dA$$

e.g. In the dilute limit: $\int_{\partial\Omega_i} -\mu(u_i n_j + u_j n_i) dA = \frac{20}{3}\pi\mu a^3 e_{ij} \quad \Rightarrow \quad \frac{1}{V}\sum \cdots = \frac{5}{2}\phi\mu e_{ij}$

$\rightarrow$ Phase-coupling in stress tensor.

[1] Balachandar & Eaton *ARFM* (2010)

Force-coupling method[2]

- Based on truncated regularized multipole expansion

$$\rho_f \left(\frac{\partial u_i}{\partial t} + u_j \frac{\partial u_i}{\partial x_j} \right) = \frac{\partial \sigma_{ij}}{\partial x_j} + \sum_n \left[F_i \Delta_M(\boldsymbol{r}) + \{T_{ij} + S_{ij}\} \frac{\partial}{\partial x_j} \Delta_D(\boldsymbol{r}) \right]^n ,$$

$$\boldsymbol{r} = \boldsymbol{x} - \boldsymbol{Y}.$$

  - $\boldsymbol{F}$: gravitational acceleration + inertia force $\rightarrow \boldsymbol{F} = \boldsymbol{F}^{ext} + (m_F - m_p)\frac{d\boldsymbol{V}}{dt}$
  - $T_{ij} = \frac{1}{2}\epsilon_{ijk}T_k$: body torque + inerital torque $\rightarrow \boldsymbol{T} = \boldsymbol{T}^{ext} + (I_F - I_p)\frac{d\boldsymbol{\Omega}}{dt}$
  - S_{ij}: surface traction $\rightarrow \int e_{ij}\Delta_D d\boldsymbol{x} = 0$

- Particle motion:

$$\boldsymbol{V} = \int \boldsymbol{u}(x)\Delta_M(\boldsymbol{r})d^3\boldsymbol{x}, \qquad \boldsymbol{\Omega} = \frac{1}{2}\int \boldsymbol{\omega}(x)\Delta_D(\boldsymbol{r})d^3\boldsymbol{x}.$$

[2] Lomholt & Maxey *JCP* (2002)

Force-coupling method[2]

- Based on truncated regularized multipole expansion

$$\rho_f\left(\frac{\partial u_i}{\partial t}+u_j\frac{\partial u_i}{\partial x_j}\right)=\frac{\partial \sigma_{ij}}{\partial x_j}+\sum_n\left[F_i\Delta_M(\boldsymbol{r})+\{T_{ij}+S_{ij}\}\frac{\partial}{\partial x_j}\Delta_D(\boldsymbol{r})\right]^n,$$

$$\boldsymbol{r}=\boldsymbol{x}-\boldsymbol{Y}.$$

  - $\boldsymbol{F}$: gravitational acceleration + inertia force $\rightarrow \boldsymbol{F}=\boldsymbol{F}^{ext}+(m_F-m_p)\frac{d\boldsymbol{V}}{dt}$
  - $T_{ij}=\frac{1}{2}\epsilon_{ijk}T_k$: body torque + inerital torque $\rightarrow \boldsymbol{T}=\boldsymbol{T}^{ext}+(I_F-I_p)\frac{d\boldsymbol{\Omega}}{dt}$
  - S_{ij}: surface traction $\rightarrow \int e_{ij}\Delta_D d\boldsymbol{x}=0$

- Particle motion:

$$\boldsymbol{V}=\int \boldsymbol{u}(x)\Delta_M(\boldsymbol{r})d^3\boldsymbol{x},\qquad \boldsymbol{\Omega}=\frac{1}{2}\int \boldsymbol{\omega}(x)\Delta_D(\boldsymbol{r})d^3\boldsymbol{x}.$$

- Mixture stress: $\sigma^m_{ij}=\sigma_{ij}+\sum S_{ij}\Delta_D$

  $\rightarrow$ Mean shear stress in a homogeneous flow

$$\tau_{ij}=-\rho_f\langle u_i'u_j'\rangle+2\mu_f\langle e_{ij}\rangle+\phi\langle S_{ij}\rangle=-\rho_f\langle u_i'u_j'\rangle+2\mu_{eff}\langle e_{ij}\rangle \quad (\because\ \langle S_{ij}\rangle\sim\langle e_{ij}\rangle)$$

  c.f. Stokes-Einstein estimate: $\mu_{eff}=\mu(1+2.5\phi)$

[2] Lomholt & Maxey *JCP* (2002)

Dissipation spectra in isotropic turbulence

- Direct numerical simulation of forced isotropic turbulence[3]

	ϕ	Re_λ	u'	ϵ	a/η	a/λ	St_l	St_K
N1	0.06	57.3	19.44	5436	5.50	0.37	0.68	10.1
N2	0.06	58.7	19.77	5574	3.84	0.26	0.33	5.0

$^*St_l = \tau_p/(u'^2/\epsilon), St_K = \tau_p/\tau_K, k_d = \pi/a$

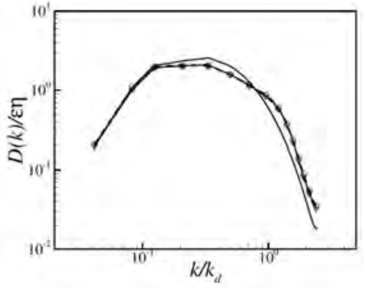

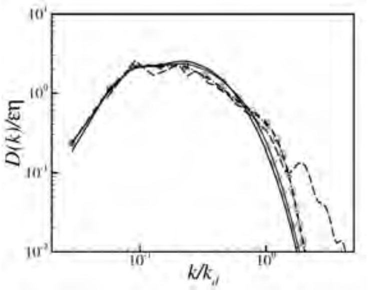

* ten Cate *et al.* (2004)

- Spectral redistribution of dissipation rate
- Significant suspension viscosity effect

[3] Yeo *et al.* *IJMF* (2010)

Spectral energy transfer by particle phase

- Energy budget

$$0 = E_{in}(k) + T(k) - D(k) + H(k)$$

$\rightarrow$ Dipole energy transfer function: $H(k) = \mathcal{F}\left\{\sum e_{ij} S_{ij} \Delta_D\right\}$

Spectral energy transfer by particle phase

- Energy budget

$$0 = E_{in}(k) + T(k) - D(k) + H(k) = E_{in}(k) + T(k) - \widetilde{D}(k) + \widetilde{H}(k)$$

$\rightarrow$ Dipole energy transfer function: $H(k) = \mathcal{F}\left\{\sum e_{ij} S_{ij} \Delta_D\right\} = -2\mu_{add} k^2 E(k) + \widetilde{H}(k)$

$\rightarrow$ Modified dissipation-rate spectra: $\widetilde{D}(k) = 2(\mu + \mu_{add}) k^2 E(k) = 2\mu_{eff} k^2 E(k)$

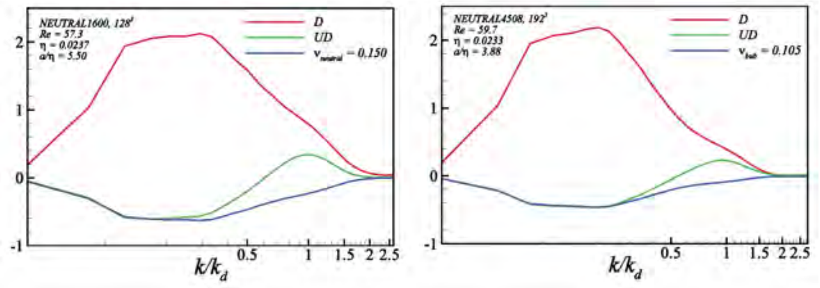

* Blue line $\rightarrow -2\mu_{add} k^2 E(k)$, $\widetilde{H}(k) = H(k) - [-2\mu_{add} k^2 E(k)]$

- $\mu_{eff} = \mu(1 + 2.5\phi)$ for larger particle, $\mu_{eff} = \mu(1 + 1.75\phi)$ for smaller particle.
- Turbulence enhancement at smaller scales
- Dipole energy transfer has a long-range effect

Kinetic Energy spectra in isotropic turbulence

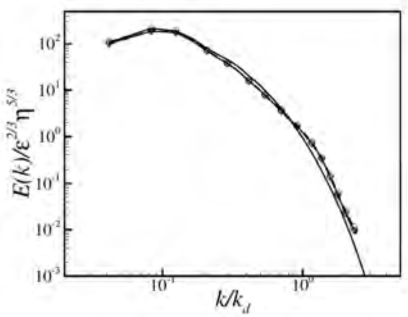

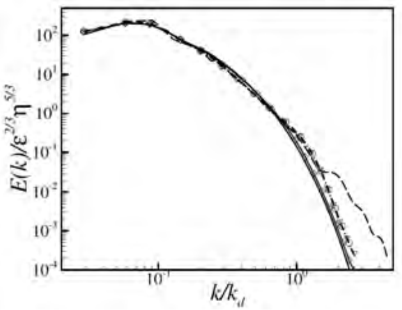

- Turbulence enhance at small scales

Preferential concentration of inertial particles

- Low inertia approximation: $0 < St \ll 1$ (Maxey 1987a,b)

$$St \frac{d\boldsymbol{V}}{dt} = (\boldsymbol{u}(\boldsymbol{Y}, t) - \boldsymbol{V}) + \boldsymbol{W}$$

$$\boldsymbol{V}(t) = \mathbf{v}(\boldsymbol{Y}, t) = (\boldsymbol{u}(\boldsymbol{Y}, t) + \boldsymbol{W}) - St\left(\frac{\partial \boldsymbol{u}}{\partial t} + (\boldsymbol{u} + \boldsymbol{W}) \cdot \nabla \boldsymbol{u}\right)$$

$$\nabla \cdot \mathbf{v} = -\frac{1}{4} St\,(\boldsymbol{e} : \boldsymbol{e} - \boldsymbol{\omega} : \boldsymbol{\omega})$$

$\rightarrow$ Effective particle velocity field $\mathbf{v}(\boldsymbol{x}, t)$ is compressible. Convergence where $|\boldsymbol{e}|^2 > |\boldsymbol{\omega}|^2$

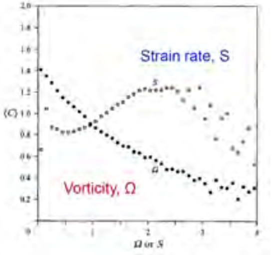

Wang & Maxey (1993)

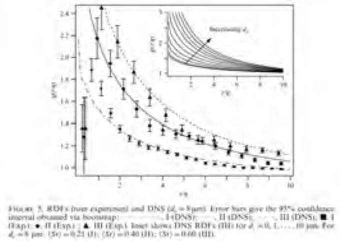

Salazar *et al.* (2008)

$\Rightarrow$ Need to consider particle-pair hydrodynamic interactions.

Particle-pair interaction

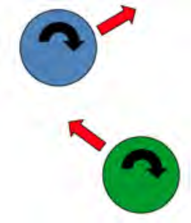

- For a gap $a\epsilon < l_{St} \sim a/Re_p$:
  $\rightarrow$ Viscous time scale $\ll$ Inertial time scale
  $\rightarrow$ Quasi-Stokes problem
  · Rapid damping of inertial acceleration
  · Coupling between particle motions

- Fundamental modes of Stokes flow
  · Particle moving relative to flow
  $u^D(\boldsymbol{r}) \sim \frac{a}{r} V$
  · Particle in a shear flow
  $u^D(\boldsymbol{r}) \sim \frac{a^3}{r^2} |\boldsymbol{e}^\infty|$

Particle-pair interaction

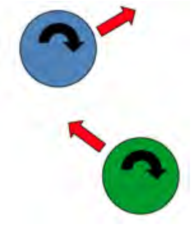

- For a gap $a\epsilon < l_{St} \sim a/Re_p$:
  - $\rightarrow$ Viscous time scale $\ll$ Inertial time scale
  - $\rightarrow$ Quasi-Stokes problem
    - · Rapid damping of inertial acceleration
    - · Coupling between particle motions

- Fundamental modes of Stokes flow
  - · Particle moving relative to flow $u^D(\boldsymbol{r}) \sim \frac{a}{r} V$
  - · Particle in a shear flow $u^D(\boldsymbol{r}) \sim \frac{a^3}{r^2} |\boldsymbol{e}^\infty|$

- hydbrid method: Ayala *et al.* (2007)

$$St\frac{d\boldsymbol{V}}{dt} = \boldsymbol{V} - (\boldsymbol{u} + \sum \boldsymbol{u}^D) - \boldsymbol{W}$$

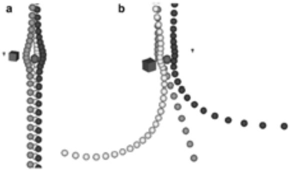

Particle-pair interaction

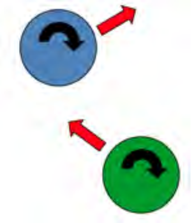

- For a gap $a\epsilon < l_{St} \sim a/Re_p$:
  $\rightarrow$ Viscous time scale $\ll$ Inertial time scale
  $\rightarrow$ Quasi-Stokes problem
  · Rapid damping of inertial acceleration
  · Coupling between particle motions

- Fundamental modes of Stokes flow
  · Particle moving relative to flow
  $u^D(\boldsymbol{r}) \sim \frac{a}{r} V$
  · Particle in a shear flow
  $u^D(\boldsymbol{r}) \sim \frac{a^3}{r^2} |\boldsymbol{e}^\infty|$
  · Particle Stress
  $S = S^\infty + S_{10} + S_{010} + \cdots$

- hydbrid method: Ayala *et al.* (2007)

$$St \frac{d\boldsymbol{V}}{dt} = \boldsymbol{V} - \left(\boldsymbol{u} + \sum \boldsymbol{u}^D\right) - \boldsymbol{W}$$

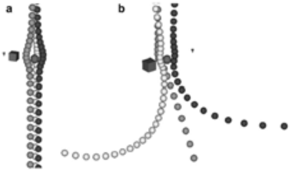

Near-field interaction

- Near-field hydrodynamic interaction

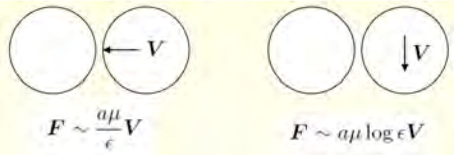

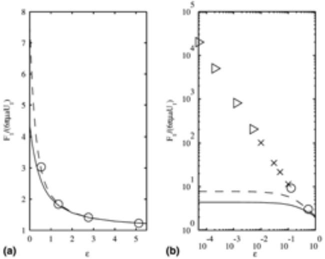

$\rightarrow$ Particle Stress: $S_{ij} \sim \frac{1}{\epsilon}$

- Non-hydrodynamic short-range interaction
  - Particle roughness element
  - Polymer coating
  - Electrostatic repulsion
  - $\cdots$

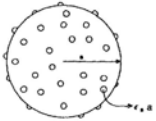

Smart & Leighton (1988)

Effects of non-hydrodynamic interaction

- Potential force model: $\boldsymbol{F}^P = -f(\epsilon)\boldsymbol{d}$ (e.g. Lennard-Jones potential, electrostatic repulsion)

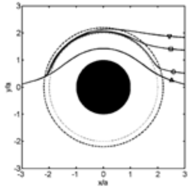

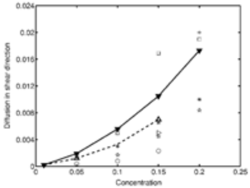

Abbas *et al.* (2006)

- Particle Stress

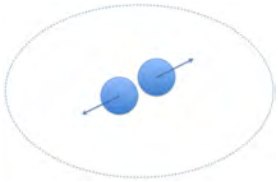

- Equal & opposite repulsive force
  $\rightarrow$ dipole force in the far-field
- Mean shear stress in a homogeneous flow
  $\tau_{ij} = -\rho_f\langle u_i' u_j'\rangle + 2\mu_f\langle e_{ij}\rangle + \phi\langle S_{ij}\rangle - n\langle \boldsymbol{R}\otimes\boldsymbol{F}^P\rangle$
- Particles in a close proximity:
  $S_{ij} \sim (1/\epsilon)\mu e_{ij}, \quad -\boldsymbol{R}\otimes\boldsymbol{F}^P \gg 2\mu e_{ij}$

- A particle doublet generates far-field dipolar flow $\rightarrow$ additional stress.
- Dissipation rate can be largely affected by RDF.

Comments so far

- Due to the separation of lengthscales, Stokesian dynamics may play a role in modeling dispersed multiphase flow
- Particle stress, or suspension viscosity, has a significant effect in turbulence modulation for $a > \eta$
- Particle stresslet as well as potential force dipole have a long-range effect and may interact with flow at a scale larger than the particle size.
- For a better prediction, a dispersed model needs to consider stress coupling between fluid and particle phases.

Background: Concentrated suspensions

- Concentrated Suspensions;
  - average separation distance is smaller than the particle size[4] ($\phi > 0.2$)
    $\rightarrow$ Nature: B'layers of density currents/ocean spray, Debris flow, Landslide
    $\rightarrow$ Engineering: Micro-bubble/emulsion DR, CHE products, medical diagnostic device

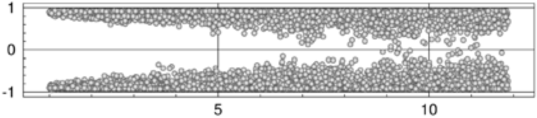

  - multiscale physics: Long-range multi-body $\sim O(10)a$
    Lubrication interactions $\sim O(10^{-3})a$
    $\Rightarrow$ No general theory
    $\Rightarrow$ Challenging both in experiments and numerical simulations
  - Non-Newtonian Rheology

[4] Stickel & Powell *ARFM* 2005

Lubrication-Corrected FCM[5]

- Multiscale computation of hydodynamic interaction
  - Far-field multibody interaction: Standard FCM
  - Near-field interaction:
    $\Rightarrow$ Pairwise-additivity of Lubrication interaction (Brady & Bossis 1988)
    - **Resistance** relation for a particle pair

$$\begin{bmatrix} \boldsymbol{F}^1 \\ \boldsymbol{F}^2 \\ \boldsymbol{T}^1 \\ \boldsymbol{T}^2 \end{bmatrix} = \mu \begin{bmatrix} \boldsymbol{A}^{11} & \boldsymbol{A}^{12} & \boldsymbol{B}^{11} & -\boldsymbol{B}^{12} & \boldsymbol{G}^{11} & -\boldsymbol{G}^{12} \\ \boldsymbol{A}^{12} & \boldsymbol{A}^{11} & \boldsymbol{B}^{12} & -\boldsymbol{B}^{11} & \boldsymbol{G}^{12} & -\boldsymbol{G}^{11} \\ (\boldsymbol{B}^{11})^T & (\boldsymbol{B}^{12})^T & \boldsymbol{C}^{11} & \boldsymbol{C}^{12} & \boldsymbol{H}^{11} & \boldsymbol{H}^{12} \\ -(\boldsymbol{B}^{12})^T & -(\boldsymbol{B}^{11})^T & \boldsymbol{C}^{12} & \boldsymbol{C}^{11} & \boldsymbol{H}^{12} & \boldsymbol{H}^{11} \end{bmatrix} \begin{bmatrix} \boldsymbol{V}^1 - \boldsymbol{V}^\infty(\boldsymbol{Y}^1) \\ \boldsymbol{V}^2 - \boldsymbol{V}^\infty(\boldsymbol{Y}^2) \\ \boldsymbol{\Omega}^1 - \boldsymbol{\Omega}^\infty(\boldsymbol{Y}^1) \\ \boldsymbol{\Omega}^2 - \boldsymbol{\Omega}^\infty(\boldsymbol{Y}^2) \\ -\boldsymbol{E}^\infty \\ -\boldsymbol{E}^\infty \end{bmatrix}.$$

    - $\boldsymbol{R} = \boldsymbol{R}^{Exact} - \boldsymbol{R}^{FCM}$: $|\boldsymbol{R}| \to 0$ for the gap between particle $\epsilon > 0.6$.
  - A coupled system of far-field and near-field interactions is solved by using a PCG.
  - Almost the same computational cost with the standard FCM,
    $\to O(N_p \log N_p)$ using a Fourier spectral method.

[5] Yeo & Maxey *JCP* (2010)

Characteristics of Concentrated Suspensions

- High-frequency viscosity
  → Monte Carlo procedure: Ensemble average of 1000 random configuration

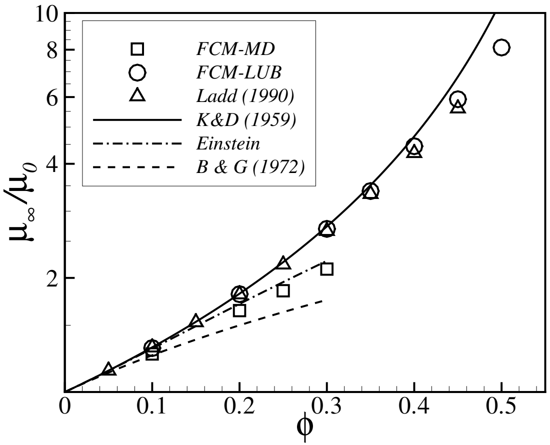

Characteristics of Concentrated Suspensions

- Stokes-flow theory:
  - Instantaneity
  - Reversible
  - Newtonian rheology

Characteristics of Concentrated Suspensions

- Stokes-flow theory:
  - Instantaneity
  - Reversible
  - Newtonian rheology

- Experimental Observation:
  - History effect
  - Irreversibility & Chaos
  - Non-Newtonian rheology

• Irreversible transition

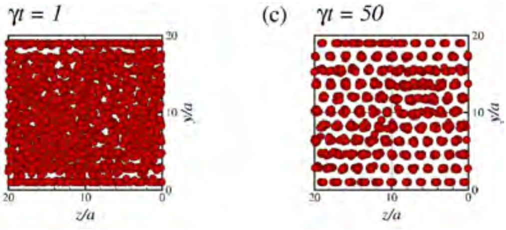

Yeo & Maxey *PRE* (2010ab)

• Particle migration

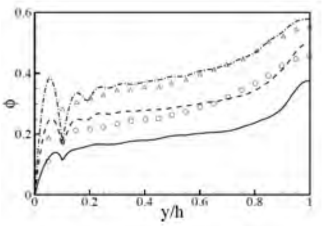

Yeo & Maxey *JFM* (2011)

Non-hydrodynamic effects

- Non-hydrodynamic interaction breaks fore-after symmetry!

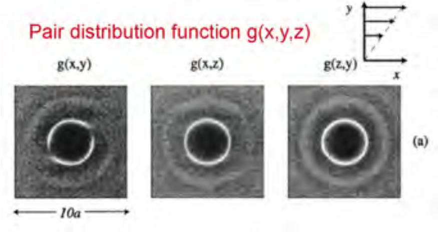

Sierou & Brady (2002)

$\Rightarrow$ Shear-induced diffusion

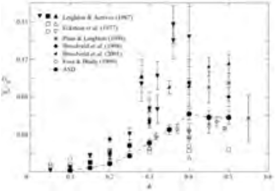

Sierou & Brady (2004)

$\Rightarrow$ Normal stress difference

$N_1 = \sigma_{11} - \sigma_{22}, N_2 = \sigma_{22} - \sigma_{33}$

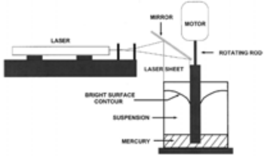

Zarraga *et al.* (2002)

Inhomogeneous suspensions

Suspensions in pressure-driven flow

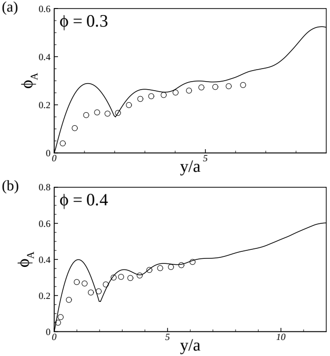

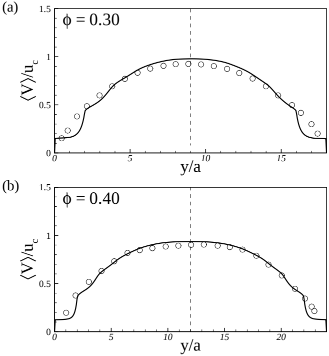

- Migration of particles: contradictory to Stokes theory
- Shear-induced migration by Leighton & Acrivos (1987)

Inhomogeneous suspensions

Suspensions in pressure-driven flow

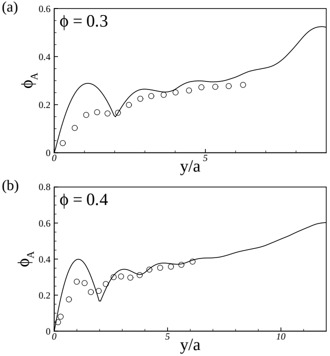

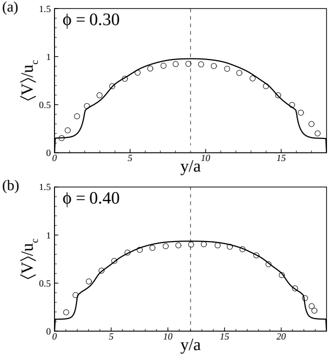

- Migration of particles: contradictory to Stokes theory
- Shear-induced migration by Leighton & Acrivos (1987)

  High shear rate: more frequent collisions

  Low shear rate: less frequent collisions

Inhomogeneous suspensions

Suspensions in pressure-driven flow

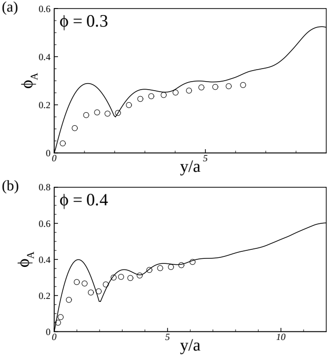

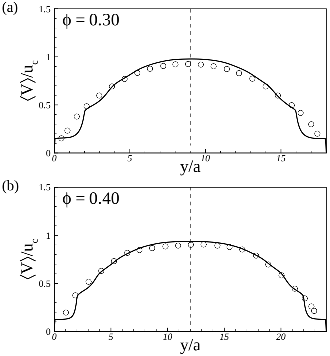

- Migration of particles: contradictory to Stokes theory
- Shear-induced migration by Leighton & Acrivos (1987)

High shear rate: more frequent collisions

$$\Downarrow \qquad j_\perp \sim \nabla\dot{\gamma}$$

Low shear rate: less frequent collisions

Particle flux model

- Shear-induced migration is a phenomenological model and unreliable for general use.
- Stress-induced migration model: based on a phase-averaged momentum conservation

[6] Morris & Boulay *JOR* (1999)

Particle flux model

- Shear-induced migration is a phenomenological model and unreliable for general use.
- Stress-induced migration model: based on a phase-averaged momentum conservation

- Particle-phase momentum conservation:[6]

$$\boldsymbol{\nabla} \cdot \langle \chi_p \boldsymbol{\sigma} \rangle - \langle \boldsymbol{\sigma} \cdot \boldsymbol{\nabla} \chi_p \rangle = 0, \quad \chi_p(\boldsymbol{x})\text{: particle-phase indicator function}$$

Local homogeneity assumption: $\boldsymbol{\nabla} \cdot \langle \chi_p \boldsymbol{\sigma} \rangle \simeq \nabla \cdot \boldsymbol{\Sigma}^P$,

$$\langle \boldsymbol{\sigma} \cdot \boldsymbol{\nabla} \chi_p \rangle \simeq -n\boldsymbol{F}^H, \quad n = \phi \times 3/4\pi a^3$$

Hydrodynamic drag model: $\boldsymbol{F}^H = -6\pi\mu a(\boldsymbol{V} - \boldsymbol{u})/f(\phi)$, $\boldsymbol{u}$: mixture velocity

Particle flux: $\boldsymbol{j} = \phi(\boldsymbol{V} - \boldsymbol{u}) = \frac{2a^2}{9\mu} f(\phi) \boldsymbol{\nabla} \cdot \boldsymbol{\Sigma}^P \Rightarrow j_\perp \sim \frac{\partial \Sigma^P_{22}}{\partial y}$

Stress modeling: Local rheology assumption

$$\boldsymbol{\Sigma}^P = \mu_f \dot{\gamma} \begin{bmatrix} p(\phi) & \mu_{eff}(\phi) & 0 \\ \mu_{eff}(\phi) & \lambda_1 p(\phi) & 0 \\ 0 & 0 & \lambda_2 p(\phi) \end{bmatrix} \quad \text{i.e.} \quad \mu_{eff}(\phi) = \left(1 - \frac{\phi}{\phi_m}\right)^{-2.5\phi_m}$$

$$p(\phi) = K \left(\frac{\phi}{\phi_m}\right)^2 \left(1 - \frac{\phi}{\phi_m}\right)^{-2}$$

[6] Morris & Boulay *JOR* (1999)

Comparison with simulations

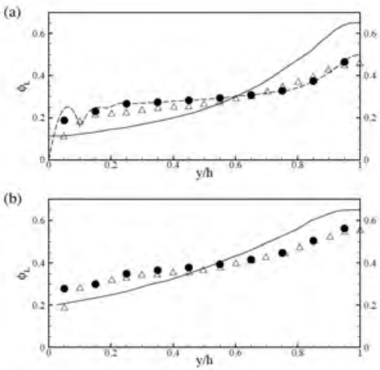

FIGURE 4. The local volume fraction profiles for (a) $\Phi = 0.3$ and (b) $\Phi = 0.4$: •, P3L and P4L; △, Gilchrist (2010); ——, Yapici *et al.* (2009). The dashed line in (a) is the area fraction (ϕ) profile of P3L.

Yeo & Maxey *JFM* (2011)

- Suspension model overestimates particle migration.

Particle normal stresses

Normal stresses, Σ_{ii}^P, scaled by the mean pressure gradient f^D and channel height h.

$\phi = 0.2$

$\phi = 0.3$

$\phi = 0.4$

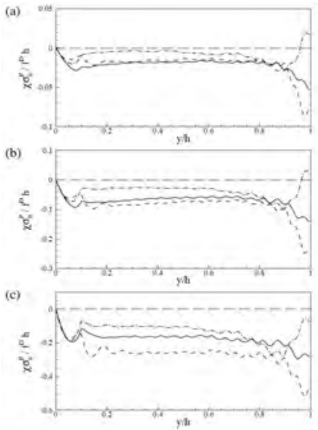

$\Sigma_{11}^P =$ ———

$\Sigma_{22}^P =$ - - - -

$\Sigma_{33}^P =$ — - —

- $\frac{\partial \Sigma_{22}^P}{\partial y} \simeq 0 \rightarrow$ consistent with the model

Particle Shear Stress

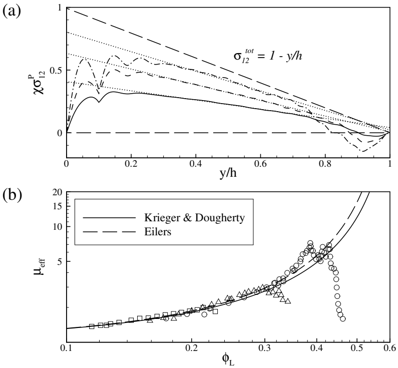

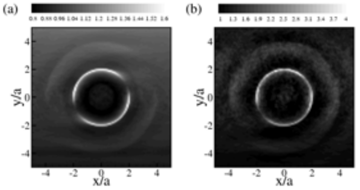

Total Shear Stress:

$$\langle \sigma_{12} \rangle = \langle \chi_p \sigma_{12} \rangle + \langle \chi_f \sigma_{12} \rangle$$
$$= \left(1 - \frac{y}{h}\right) f^D h.$$

Effective Viscosity:

$$\frac{\mu_{eff}}{\mu_0} = \frac{\langle \sigma_{12} \rangle}{\langle \chi_f \sigma_{12} \rangle}$$
$$= 1 + \frac{\langle \chi_p \sigma_{12} \rangle}{(1 - y/h) f^D h - \langle \chi_p \sigma_{12} \rangle}.$$

- Local Rheology assumption is valid.
- Suspension microstructure changes near the center.
- Significant non-local effects in the channel center.

Time & Length scales of concentrated suspension

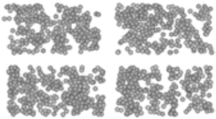

Melrose & Ball (2004)

- Stokes theory: fixed timescale ($\dot{\gamma}$) & lengthscale (a)
- Concentrated suspensions:
  Formation of hydro-cluster introduces time & lengthscales

- Hysteresis

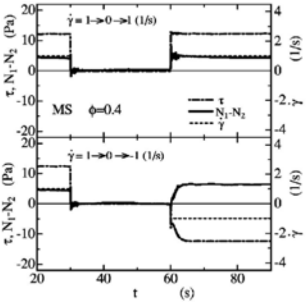

Narumi *et al.* *JOR* (2002)

- Lengthscales

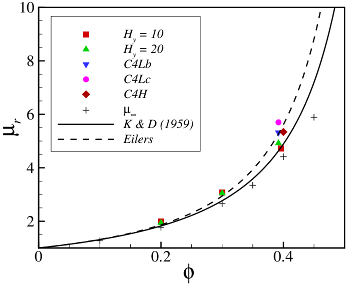

Yeo & Maxey *JFM* (2010), *Europhys. Lett.* (2010)

Suspensions in uniform shear flow: $Re_p > 0$

- Stokes suspensions: theoretical study, relevant to microfluidic devices, CHE products
- Mechanical/Natural flow systems of interest: $0 < Re_p$

$\Rightarrow$ What is the effect of finite inertia on dynamics of concentrated suspensions?

- Particle-pair interaction revisited.

Stokes flows

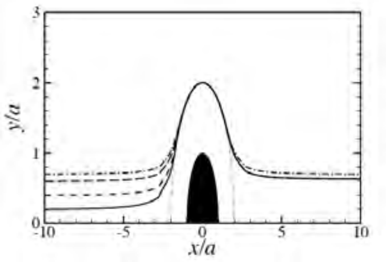

$Re_p = 1$

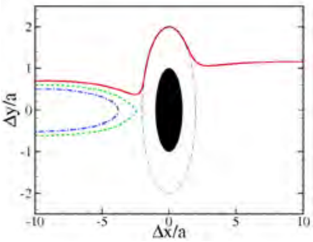

- $Re_p > 0$ introduces irreversibility to flow, beyond that due to contact forces
- At $Re_p > 0$, particle-pair interaction is sufficient to generate diffusive motion

Effective viscosity

Effective shear viscosity

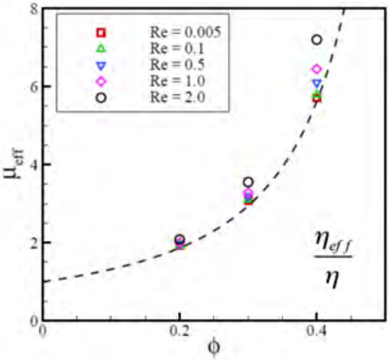

Particle shear stress v.s. Re_p

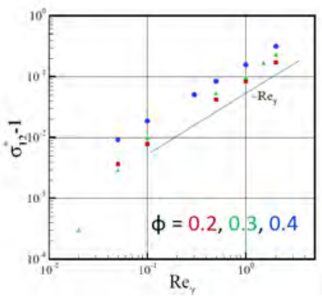

- Finite-Re_p suspension is shear-thickening. → stronger shear, higher viscosity

Velocity fluctuations and PDFs [7]

$\phi = 0.2$

$\phi = 0.4$

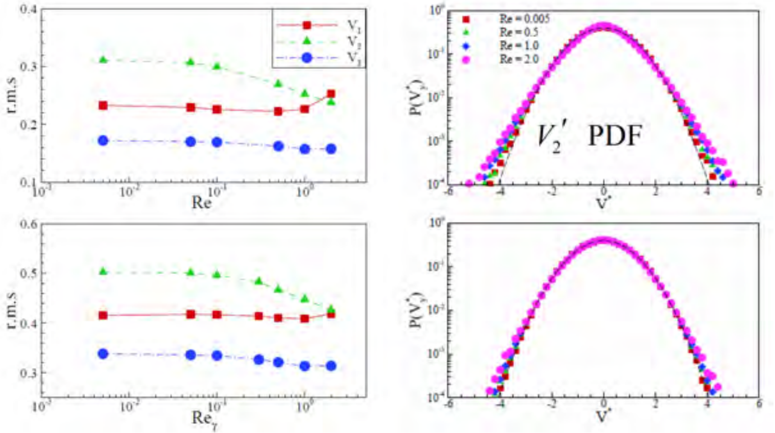

$\frac{V'}{a\dot{\gamma}}$ vs Re_p

$V^* = \frac{V_2}{\sigma_2}$

- Kinetic Energy of the particle phase decreases at higher Re_p
- Flatness increases slightly with Re_p

[7] Yeo & Maxey *POF* in review

Cross-flow diffusion

Diffusivity ($D_{ii} = V'^2_i \int \rho(\tau) d\tau$)

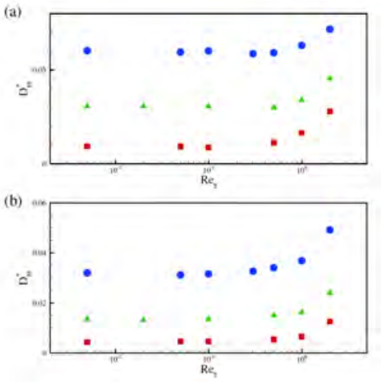

■ $\phi = 0.2$, ▲ $\phi = 0.3$, ● $\phi = 0.4$

- Diffusivity is an increasing function of Re_p, while the velocity fluctuation decreases at higher Re_p.

Cross-flow diffusion

Diffusivity ($D_{ii} = V'^2_i \int \rho(\tau) d\tau$)

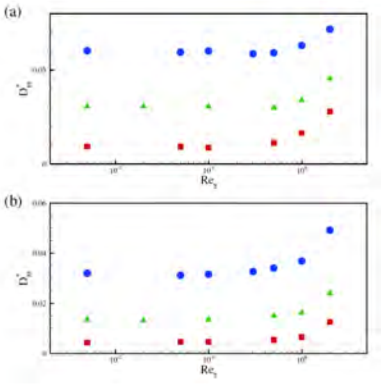

■ $\phi = 0.2$, ▲ $\phi = 0.3$, ● $\phi = 0.4$

Mean-square displacement

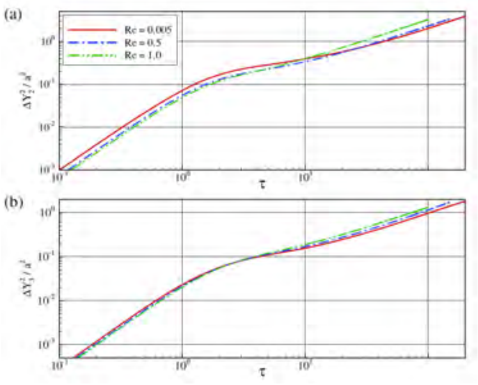

$\phi = 0.2$

- Diffusivity is an increasing function of Re_p, while the velocity fluctuation decreases at higher Re_p.
- At higher Re_p, the reduced intermediate region results in the increase in D_{ii}.

Lagrangian auto-correlation

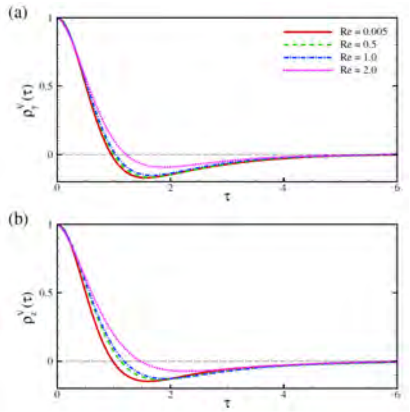

- Decreased negative loop $\rightarrow$ longer correlation $\rightarrow$ larger T_L $\rightarrow$ increase in D_{ii}
- Longer-time tail ($\tau > 3\dot{\gamma}t$) collapes onto one curve.

Pair-distribution function in the plane of shear: $g(r, \theta, 0)$

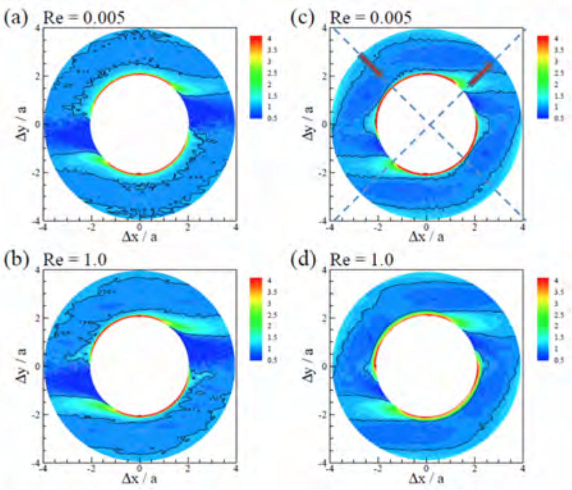

Principal Axis

- Earlier detachment reduces the negative correlation.
- Increase inertia → increase in the wake region
- Far-field PDF is less sensitive to inertia.

Near-contact pair distribution function

Near contact PDF

PDF weighted by S_{12}

$\phi = 0.2$

$\phi = 0.3$

$\phi = 0.4$

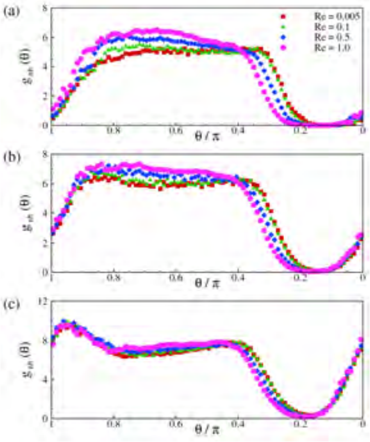

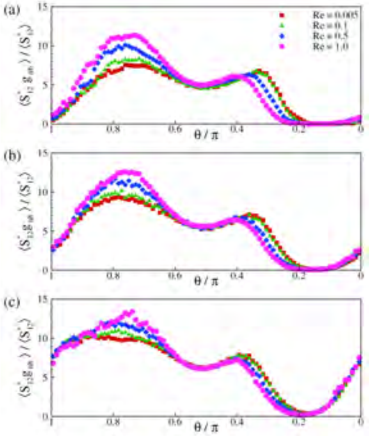

- Detachment point moves towards upstream
- Increased contributions from the compressible pricipal axis events ($\theta/\pi = 0.75$)

Intermittency of particle shear stress

$$S_{12} = \text{hydrodynamic + potential force}$$
$$= S^H_{12} - \tfrac{1}{2}\sum \boldsymbol{r} \otimes \boldsymbol{F}^P$$

$$S^*_{12} = \frac{S_{12} - \langle S_{12}\rangle}{\sigma_S}$$

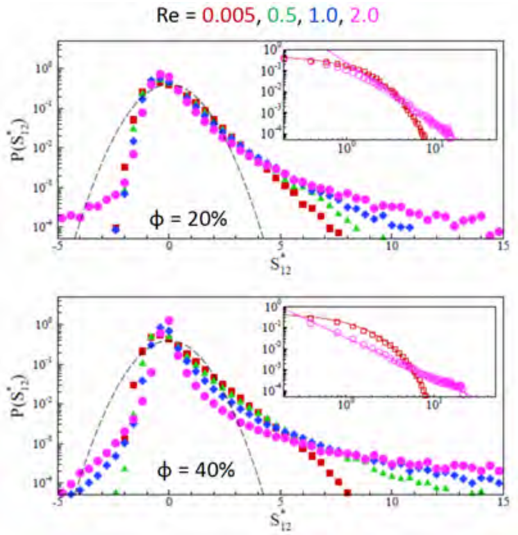

- Exponential decay at low Re_p
- Algebraic decay at higher Re_p

Summary

- Dispersed multiphase flow is a good example of multiscale physics. For a better understanding we need to gather information scattered across disciplines from microhydrodynamics to turbulent flows.
- Phase-coupling in stress tensor has a significant effect on turbulence modulation. For a better estimate of the stress coupling, not only stress re-distribution around an isolated particle, but also particle-pair dynamics needs to be accurately resolved.
- To develop a self-consistent multiscale model, there is a need to incorporate well established results of dense suspensions in CHE into the study of multiphase flow in the boundary layer.
- Dense finite-inertia suspension flow is a grey area, which is not well understood.